Analytical Pyrolysis Letters
Volume APL009, page 1-11
Published 28/07/2023

APL
ISSN: 2659-5605

Molecular characterization of Asian hornet paper envelope nests

Joeri Kaal [a,*], Luis Rodríguez-Lado [b]
[a] Pyrolyscience, Madrid–Santiago de Compostela, Spain
[b] GeoForsk, Escultor Ferreiro 9 2º, Noia, 15200 Spain. luisrlado@gmail.com

*** Corresponding author email address**: joeri@pyrolyscience.com

Abstract

We explored the potential of pyrolysis-gas chromatography-mass spectrometry (Py-GC-MS) as a molecular characterization tool for paper envelop materials in nests of the Asian hornet (*Vespa velutina* Lepeletier, 1836), a runaway invasive species in Western Europe. The area of study is the NW of the Iberian Peninsula (Galicia, A Coruña province) and the main tree types of the vegetation in the sampled areas are pine, eucalypt and oak, with a smaller abundance of chestnut and fruit trees. The objective was to determine whether molecular fingerprinting in combination with the information on vegetation patterns allows to determine the origin of the decaying wood fibres used for nest construction, and thereby determine the insects' preferences for raw material. The results confirm that the envelopes consist predominantly of polysaccharides and lignin, and that especially the lignin composition is useful for tracking vegetation sources of raw materials. The relationships between dominant vegetation and nest composition was smaller than expected and there seems to be no clear preference for a given tree type, in spite of very large inter-nest variation in the balance between guaiacyl and syringol lignin products (S/G ranging between 0.0 and 3.0). Thus, the Asian hornet does not exhibit a specific preference for a particular type of vegetation. Instead, it adapts to the available materials in its environment and uses them conveniently in nest construction. This highlights the high flexibility of the Asian wasp in utilizing the resources of the environment it colonizes. However, remarkable intra-nest variation in both colour and S/G ratio indicates that nest colour banding is related to raw material selection. This study contributes to a better understanding of the behavior of *V. velutina*, which, in turn, helps define appropriate actions to limit its expansion.

Keywords: Asian hornet, paper nest envelopes, molecular characterization, Py-GC-MS, insect ecology.

1. Introduction

The invasion of Western Europe by *Vespa velutina* (Hymenoptera: Vespidae), subspecies *V. velutina nigrithorax* Buysson, 1905 (from hereafter *V. velutina*) started in or shortly before 2004 in SW France (Rome et al., 2013). It is a significant threat to biodiversity, food web structure, ecosystem services, socio-economical sectors –e.g. beekeeping, viticulture and fruticulture, as the species preys upon honeybees and other crucial insect pollinators (Rodríguez-Flores et al., 2019; Feás and Charles, 2019)–, and poses a direct threat to human safety, especially in rural zones and rural-urban interfaces along the Atlantic coast. Most countries in Western Europe consider the strategies to mitigate the phenomenon as failed; eradication is considered impossible (Pazos et al., 2022). Hence, management is now concentrating on the removal of the nests of hornet colonies in close proximity to the human population, to avoid attacks on humans.

The architecture of the nests of social wasps and hornets includes several main parts, i.e. pedicel (tissue that connects the nest to the substrate), envelope (papery exterior material) and combs (interior structure of hexagonal brood cells, where eggs are deposited and the larval/pupal stages are completed) (e.g. Wenzel, 2020). The envelope is composed of lignocellulosic fibres that are ground by the mandibles and mixed with its proteinaceous saliva (as an adhesive) by the pulp forage workers, and then distributed by the builders. The pedicel is composed of polysaccharides and salivary proteins. Combs may contain a silken cap (residues of pupation) and meconium (faecal waste of larvae). With exception of the meconia, the nests usually remain "clean" throughout their use cycle, as the envelopes protect the nests from biological attack and *V. velutina* does not use the nests to store food (Schmolz et al., 2000). This facilitates straightforward molecular characterization of the nests' constituents.

At present, there is a lack of fundamental knowledge about biological factors that influence the behaviour of *V. velutina* (Feás and Charles, 2019). Here we explore the potential of molecular characterization of *V. velutina* nest materials as a source of information on the ecology of *V. velutina* in relation to its natural environment. In particular, we study the mechanisms that control the variation in the organic macromolecular chemistry of the paper envelopes of the nests. We also explore the usefulness of analytical pyrolysis techniques for molecular characterization of nest materials. These techniques are scarcely used in applied entomological research, and as far as we know has never been used for the study of eusocial insects' paper envelopes. We hypothesize that the hornets gather material from nearby tree communities, that local vegetation controls the chemical features of the paper envelopes, and that analytical pyrolysis is a useful tool for molecular provenancing of building materials.

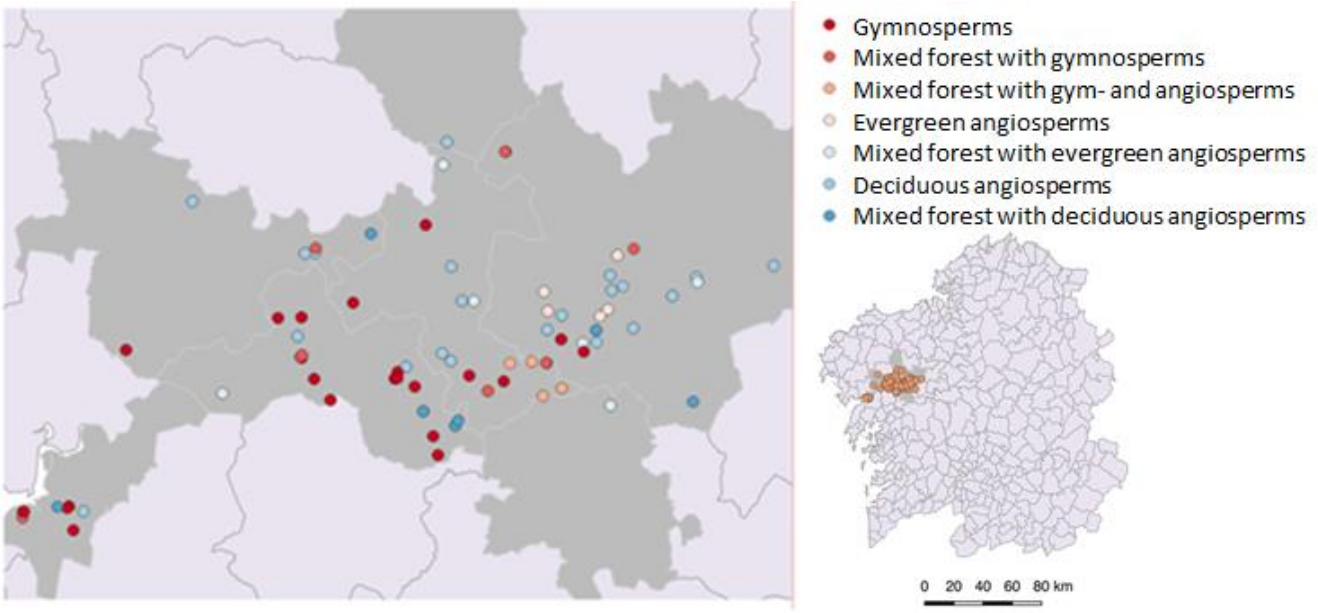

Figure 1. Location of the study area in Galicia (NW Spain). Dots mark the sampling sites. Colour indicates the surrounding vegetation.

2. Material and Methods

2.1. Sample collection and preparation

Even though recently drones equipped with flamethrowers are employed for the removal of nests, the most common method is physical removal, often by firefighters. This is also the case in Galicia (NW Spain), where the mild winter temperatures, high precipitation and humidity, and vast forested areas create the ideal environment for the Asian yellow-legged hornet. In Galicia, colonies established since late 2012 (Rome et al., 2013; Rodríguez-Flores et al., 2018), and tens of thousands of nests are destroyed each year.

The collection of nests was carried out in 2018 (July 2nd to August 22nd), in a 30 km W-E transect in the province of A Coruña, from the coast near Noia to Santiago de Compostela (climatic gradient). The transect includes the municipalities of Noia, Negreira, Brión, Ames, Santiago de Compostela, Val do Dubra and Teo (**Figure 1**). This isn an area with a high incidence of Asian hornets. Due to the danger in the handling of the nests, the collaboration of the Santiago Fire Service, the Brión GES and the Ames Council was required. They provided samples of the nests removed in their jurisdictions. Most of the nests were located in or near buildings, a bias that derives from the fact that the location of the collected nests comes from citizen requests for removal to the relevant alert services. In total, 82 samples of nest envelopes were collected, of which 5 were discarded for containing exclusively pedicel and primary nest materials, or abundance of dirt that could distort the molecular signals. Hence, a

total of 77 nest envelope samples were analysed in this study.

The samples were georeferenced and prepared for subsequent analysis (surface cleaning to remove impurities from plant remains, removal of larvae and adults still present in the nests; air-drying for a week prior to their storage for their analysis in the laboratory). For selected samples, nest sections other than the envelope were prepared as well.

The envelopes of the nests are characterized by a series of bands of different colour (horizontal stripes), in the ranges of white-cream, yellowish, purple and dark brown. The pattern of narrow horizontal stripes is the result of "edge-building" technique of the builders (Wenzel, 2020), with each band corresponding to the material collected by an individual or perhaps small group of pulp foragers, collecting plant fibres from the same source. The internal nest diversity observed with the naked eye could have its correspondence also at the level of molecular composition and introduce a variation factor that would difficult the interpretation of the results. Therefore, the variation in envelope chemistry was studied for a sample with clear band patterns (sample #48; **Figure 2**). For this sample, a joint sample of 4-5 cm^2 (25 mg) was analyzed that included all visible bands and respecting the proportionality of total variation in the nest, and material was also analyzed separately from the dark-, red- and white-coloured bands (**Figure 2**). For the remaining nests, only the composite samples were analyzed. In selecting the sample area, materials from primary nests, materials close to the overlap of the different layers of the envelope (thicker and more viscous than the surface material) and materials close to the orifice or the pedicel were avoided.

2.2. *Pyrolysis-GC-MS*

The samples were crushed and ground with a manual agate mill until they were transformed into a particulate material with a homogeneity that was judged suitable for analysis.

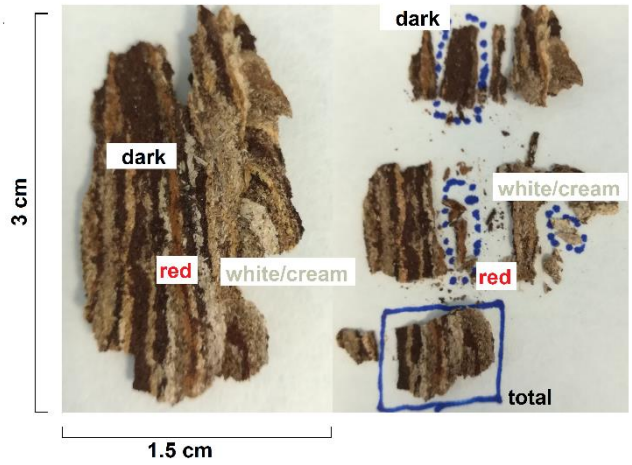

Figure 2. Striped pattern of a paper envelope subsample with a particularly marked pattern and with abundant dark- and red-coloured sections.

Pyrolysis-GC-MS was performed using an Agilent 5975 GC-MS system coupled to Pyroprobe 5000 pyrolyzer (Kaal et al., 2020). For each nest, approximately 0.5 mg of ground material was introduced into quartz tubes that were previously deactivated by combustion at 900 °C in a Lenton muffle furnace. The pyrolysis was carried out in a CDS Analytical pyrolyzer (model Pyroprobe 5000) at 650 °C set-point temperature using a temperature ramp of 10 °C/ms. The pyrolysis temperature was maintained for 20 seconds. For one sample, the proportion of mass lost by pyrolytic reactions was measured by weighing. In this case, the initial weight introduced was 0.6 mg, of which 85% was converted to gases in the pyrolysis process. Indeed, qualitatively, it was observed that all the samples had very low carbon (carbonization) and tar (condensation) residues, especially compared to the pyrolysis of their main original raw material, i.e. wood. Inorganic ash seems to be absent in its entirety, which indicates that the data generated are representative of the contents of the samples.

The pyrolyzer interface was at 325 °C. The separation of pyrolysis products was performed using an Agilent Technologies gas chromatograph (Model 6890), with the following parameters:

- Initial oven temperature = 70 °C
- Temperature ramp 1 = 20 °C /min up to 200 °C
- Temperature ramp 2 = 50 °C /min up to 325 °C

- Final temperature = 325 °C maintained for 1 min.
- Temperature of the chromatograph injector = 325 °C
- Chromatograph injector mode: splitless
- Chromatographic column: HP5-MS (non-polar).

The interface between the chromatograph and the mass spectrometer (Agilent Technologies, Model 5975) was held constant at 325 °C. The detector scanned in the *m*/*z* range of 50–500.

Each of the pyrolysis chromatograms (pyrograms) obtained was visually evaluated, recording the main peaks and generating a list of 42 pyrolysis products (**Appendix 1**). The relative proportions of these compounds were calculated based on the areas of their main *m*/*z* fragments.

The methodology of safely obtaining the nests, with the extraction by the corresponding services, means that the collected material sometimes had molecular signs of the insecticides used to inactivate the nest. The analyses indicate specifically the presence of insecticides based on piperonyl butoxide chemicals. The pyrolysis products of these insecticides (compounds with a 1,3-benzodioxole backbone) and piperonyl butoxide itself were not included in the analysis. In this study, terpenes were not evaluated either.

Selected samples were also analysed by thermally assisted hydrolysis and methylation (THM-GC-MS), to obtain additional information on lignin, tannin, fatty acid and resin composition (Challinor, 2001; Kaal et al. 2017).

2.3. *Vegetation patterns*

The existing vegetation around the nests was established using the cartography of the Land Use Information System in Spain (SIOSE) at a scale of 1:25000. This cartography, in digital format, represents polygonal land use units linked to a database that indicates the proportions of the different types of vegetation present in the unit. Because the priority construction material is plant material, for each nest, the forest unit closest to the nest was determined using SIOSE. The distances from the forest masses to the nests varied from 0 to 760 meters, with an average distance of 160 meters. The typology of nests was simplified based on the cumulative percentage of surface in: gymnosperms (mainly pines), evergreen angiosperms (mainly eucalyptus), deciduous angiosperms (oak, chestnut, etc.), mixed forests with an abundance of gymnosperms, mixed forests with an abundance of evergreen angiosperms, mixed forests with an abundance of deciduous angiosperms and mixed gymnosperm and angiosperm forests (**Figure 1**). A second level of simplification was used to differentiate angiosperm, gymnosperm and mixed forests.

2.4. *Data evaluation*

A Canonical Partial Least Squares ('plsca') analysis was performed to study the relationship between the molecular composition of nests and vegetation. This is a multivariate method that allows the investigation of relationships between two blocks of data, X and Y, assuming a symmetrical role between both blocks. In other words, neither block can be considered solely as a predictor variable or a response variable; instead, both sets of data are treated as descriptors of a shared reality. The 'plsca' model synthesizes the information from the two blocks into a series of new variables known as latent variables, which summarize the information contained in both datasets. Visualizing the scores of each variable on the main latent variables, in the form of a circle of correlations, facilitates the interpretation of the covariance relationships between the parameters of both data sets. In this case, the 'plsca' model was created using as blocks the molecular composition of the nests (X) and the predominant vegetation types in the vicinity of the nest (Y).

3. Results and Discussion

3.1. *Different parts of the nest*

The pyrolysis fingerprints of the nest sections were clearly different (see also Schmolz et al., 2000, based on thermogravimetry). The combs gave large peaks for protein compounds (ethylpyrrole, indole, 4-methylindole) and other N-containing compounds (*m*/*z* 56+151+166, *m*/*z* 56+111+126) (not shown), associated with the presence of silk and perhaps chitin from the larval pupae. The meconium (detrital materials of the larvae; **Figure 3**) samples were similarin composition to the combs, with a high abundance of chitin markers, but with a higher

proportion of polysaccharides. The pedicel has a pyrolytic signal very similar to that of the nest envelopes (see below), with no evidence of a major salivary component, as opposed to pedicels of nests of wasps such as *Polistes annularis*, which has a N-rich pedicel (Espelie and Himmelsbach, 1990).

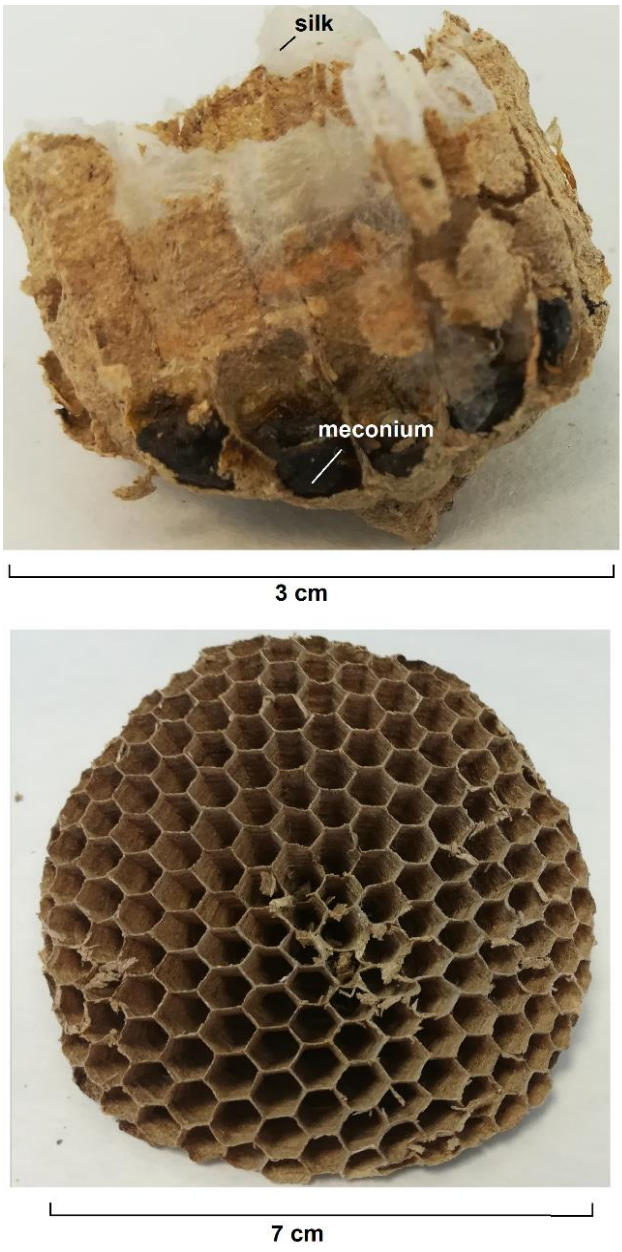

Figure 3. Comb structure showing thick deposits of meconium and silken residues in the brood cells (upper photograph) and the comb structure of a largely empty panel).

From these analyses it was concluded that the interior of the nests contains materials derived from protein, chitin and other N-rich biocomponents, the products of which were virtually absent in the pedicel and paper envelope samples, which are composed predominantly of plant fabric. Since the aim of the study was to determine the relationship between the molecular composition of nests and vegetation environment, the remainder of this article is dedicated to the paper envelopes.

3.2. *Different sections of the nest envelope*

Most nests show a striped colour pattern ranging from white to dark brown (**Figure 4)**, including cream-coloured yellowish and reddish materials. Separate analysis of different parts of one sample (sample #48; **Figure 2**), showed that the white/cream-coloured material contained much more syringyl lignin than the red- and brown-coloured bands (not shown). More specifically, the distribution of compound groups is as follows: carbohydrates (white > dark > red), guaiacyl lignin (red > dark > white), syringyl lignin (white > red > dark), and phenols (dark > red > white). The S/G ratio (lignin composition parameter; Hedges and Mann, 1979) of the "total" sample is 0.35, which is intermediate to the values of 0.11 (red), 0.15 (dark) and 0.55 (white). Such a large difference can only be explained by differential source collection by the pulp foragers.

The variability in S/G is related to the different metabolic types of shikimic acid and is representative of the type of raw material used in the nests. The results of the sample #48 can be explained by two main sources of variation in lignin composition of woody plants. Firstly, gymnosperms do not metabolize syringyl lignin, so that the dark- and red-coloured bands, with very low S/G, may correspond to gymnosperm material (mostly pine stands in the study area), whereas the S-rich white/cream-coloured materials would have been collected from angiosperm trees (e.g. deciduous oak and eucalypt in the study area). Most shrubs and herbs also produce S and G lignin. Secondly, within some, yet not all (Neiva et al., 2020) angiosperm tree woods, bark and cork materials have G-dominated lignin whereas xylem has the typical G and S co-occurrence (Lourenço et al., 2016). Thus, it may be that for dark-/red-coloured paper materials, bark materials were selectively collected.

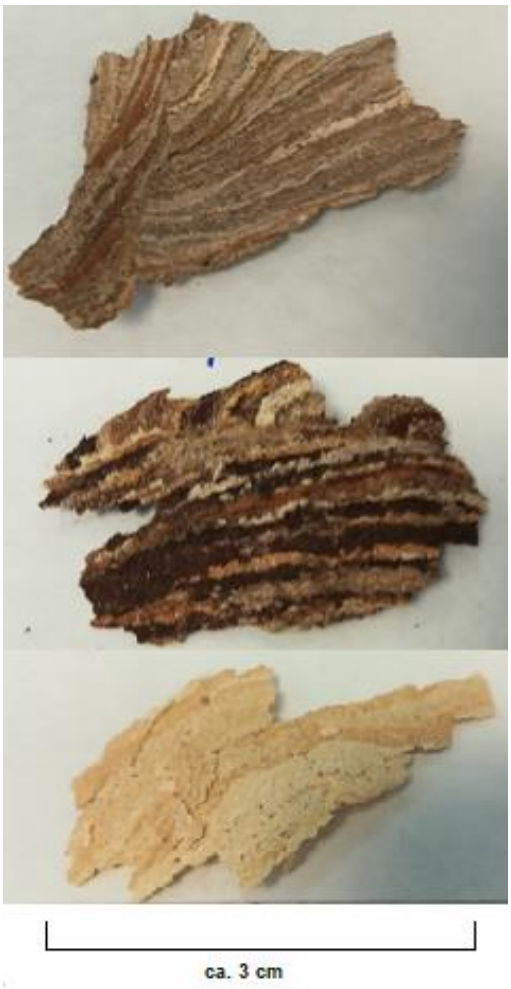

Figure 4. Examples of paper envelope materials with different colour patters.

Some additional observations allow us to hypothesize on the cause of the variation in the S/G ratio. Firstly, the total absence of 4-vinylphenol in the samples suggests that *V. velutina* does not collect herbaceous raw material. Therefore, all the material in the envelopes originates from trees and shrubs (or woody construction materials made thereof). Secondly, bark material is not likely to be used, as indicated by the THM-GC-MS analysis of selected samples, which did not show the presence of suberin (not shown), a macromolecule that is highly abundant in suberized tissues such as bark. Consequently, it appears more likely that the color of the stripes is related to the alternative use of materials from angiosperms and gymnosperms in the construction of the nest, although a combined influence cannot be ruled out.

Nevertheless, any sample with S/G > 0.8 must consist mainly of wood pulp collected from angiosperm tree xylem.

This question can probably be resolved by performing a more thorough analysis of the pyrolysis chromatograms (we studied only 42 products), especially when resin materials are included in the study, and a more detailed assessment of envelope composition using THM-GC-MS.

3.3. Variation in molecular properties of envelope material

The main pyrolysis products identified in the 3-4 cm^2 composite samples of nest envelopes are derived from lignin and polysaccharides (**Appendix 1**).

The most abundant products are the polysaccharide-derived levoglucosan (20.0 ± 8.1 % of TQPA) and acetic acid (16.2 ± 7.0 %). The sum of all carbohydrate products (acetic acid, furans, pyrans, cyclopentenones and anhydrosugars) is 61.1 ± 8.5 % (**Table 1**), showing the predominance of polysaccharides (holocellulose) in the paper envelope materials, which is in agreement with previous studies (Espelie and Himmelsbach, 1990; Schmolz et al., 2000). The salivary constituents may contribute to the carbohydrate product group, but the very weak signals of proteins and mucus (saliva is a chitin-like secretion mainly composed of a proline-rich protein) suggests that saliva has only a very minor contribution to the pyrolysis fingerprint of the paper envelopes, that can only be quantified based on minor compounds not used in this study.

Table 1. Py-GC-MS compound group sums with average (*n*=77) contributions to the paper envelope samples pyrolysis signal, and standard deviations (SD). The syringyl to guaiacyl ratio (S/G) of lignin products is also shown.

Group	% (average)	SD
Carbohydrates	61.11	8.48
Lignin (G)	15.03	6.32
Lignin (S)	14.80	7.27
Phenols & catechols	6.58	2.04
Fatty acids	0.82	0.53
others	1.66	0.48
S/G ratio	1.16	0.65

Most other pyrolysis products can be attributed to lignin, either unequivocally (methoxyphenol products, from guaiacyl and syringyl moieties) or with strong likelihood (phenols, catechols). These compounds combined account for 36.4 ± 8.6 % of the pyrolyzate signal. Major guaiacol products (15.0 ± 7.3 %) include guaiacol, 4-methylguaiacol, 4-vinylguaiacol and propenylguaiacols. Analogous compounds have been identified among the major syringols (14.8 ± 7.3%). It is striking that 4-vinylphenol, a major product of herbaceous lignin, was below the detection limit, showing that decaying grass is ignored by *V. velutina* during raw material collection. Note that not all social wasps build lignin-containing envelopes (Schmolz et al., 2000; based on thermogravimetry).

Fatty acids account for 0.8 ± 0.5%. Unidentified compounds (0.8 ± 0.1%) are probably derived from polysaccharides. Thus, the envelopes are composed almost entirely of lignin and polysaccharides (traces of resin were not considered), and the analysis of the variability between samples was focused on the lignocellulose components.

The S/G ratio ranges from very low values of <0.05 (almost exclusively G lignin) to values exceeding 2.5 (dominant S lignin). Many nest samples have S/G ratios exceeding 1.5 (n=21), and even 2.0 (n=12). These values indicate the predominant use of angiosperm raw material, and also of angiosperms with a high S/G ratio such as eucalypt wood. Indeed, S/G is a key factor controlling lignin structure in hardwoods (Santos et al., 2012), and the wide range in S/G of the samples implies a potential for hardwood tree source identification from envelope analysis. Another series of samples has an S/G ratio below 0.5 (n=11) or even 0.2 (n=5), which indicates that the material of these samples comes almost exclusively from gymnosperms and/or bark material.

There is no clear relationship between S/G and nearest forest vegetation type (**Figure 5**). The S/G ratio alone does not explain the relationship between nest composition and surrounding vegetation typology. .For instance, nests #7 #9, #16, #30 and #68 have a high S/G ratio but the surrounding vegetation is gymnosperm-dominated, and samples #19, #24, #25, # 64 and #72, with low S/G, are nearby angiosperm vegetation. Indeed, the ANOVA analysis between each of the components separately and the vegetation do not show significant relationships, suggesting that other factors control raw material selection. It is well-known that *V. velutina* uses not only natural forest as the source of wood pulp.

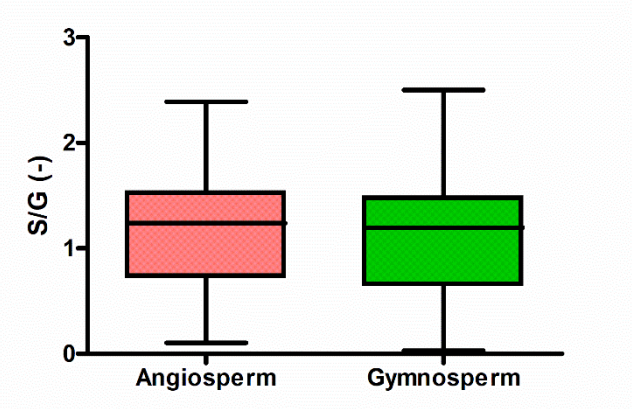

Figure 5. Simplified parameter of natural vegetation surrounding a paper envelope sampling site and the syringol/guaiacol (S/G) ratio of its lignin. Variation within the two main vegetation types is very large (no significant difference in S/G).

However, there is a weak link between the S/G ratio of the samples obtained from the gymnosperm-dominated zones and the distance to the nearest forest unit, with lowest S/G in general coinciding with samples in close proximity to pine stands (P<0.01; **Figure 6**). This may explain the lack of a clear link between S/G and vegetation: low S/G near pine-dominated woodland is only detected wheen the nest was in close proximity of the forest stand. When the distance is more than a couple of 100 m, selection of gymnosperm wood for nest construction is not detectable.

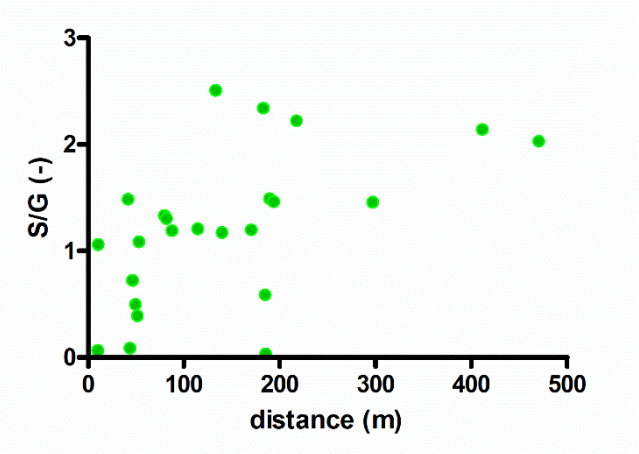

Figure 6. Relationship between the distance of a paper envelope sampling site to the nearest vegetation unit and the S/G ratio, for samples in proximity of pine-dominated woodland.

The determination of parameters indicative of the state of wood preservation (SWPI-G = 0.02 ± 0.01, SWPI-S = 0.01 ± 0.00, SWPI-Ps = 0.79 ± 0.11; Traoré et al. 2017) shows that the values are very high, in the ranges of living wood, without a clear indication of general degradation. Oxidation ratios of lignin side chains such as 4-acetylguaiacol/total guaiacols (0.08 ± 0.03) and 4-acetylsyringol/total syringols (0.06 ± 0.02) are low, confirming intact lignin. Social wasps and hornets collect slightly rotten thoroughly chewed wood (Schmolz et al., 2000), but the lignin is apparently well-preserved on the molecular level and probably indicates that the species is using rather fresh materials. This also implies that lignin composition can be used as a proxy of provenance, but for that purpose a reference database of regionally important vegetation (especially angiosperms) would be needed.

3.4. Multivariate analysis between the molecular composition of the nests and predominant vegetation.

The Canonical Partial Least Squares ('plsca') analysis was performed to study the relationship between the molecular composition of nests and vegetation. **Figure 7** shows the circle of correlations between the detected compounds and the predominant vegetation type. We observe that axis 1 discriminates between the compounds derived from polysaccharides and fatty acids, with negative contributions on this axis, and the compounds derived from lignin (guaiacols and syringols), with positive contributions. Axis 2 discriminates the molecular composition of lignin compounds, with guaiacols in the positive part and syringols in the negative part.

There is a clear correlation between the presence of guaiacols and pine forests (CNF), well-differentiated in the upper right quadrant of **Figure 7**. This indicates that the nests in pine environments contain more lignin and in particular G-type lignin, corroborating the finding that S/G is influenced mainly by vegetation type. Thus, *V. velutina* seems not to use bark as forage material. The units of deciduous hardwoods (FDC) and evergreen hardwoods (FDP) appear segregated in the lower quadrants of the figure, associated with syringyl lignin. However, the greater presence of compounds derived from polysaccharides in evergreen broadleaf forests (FDP) causes this unit to appear displaced towards the lower left quadrant of the graph (**Figure 7)**.

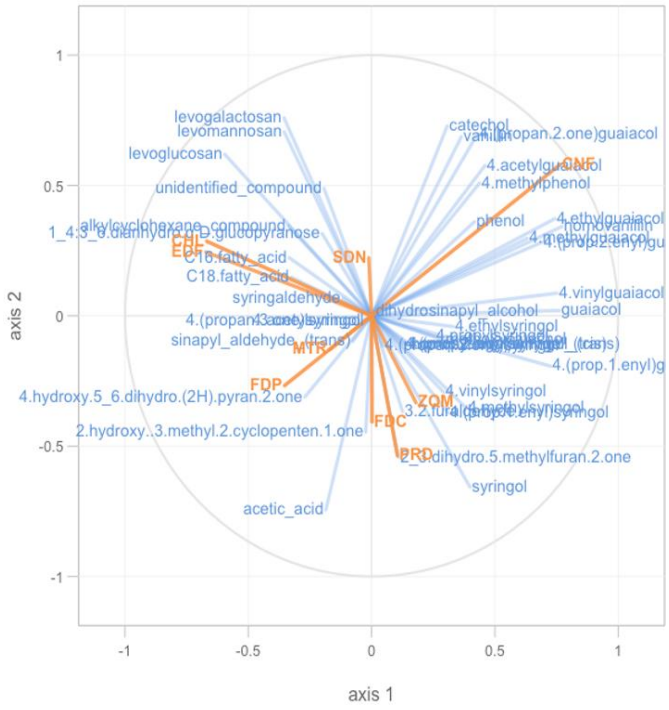

Figure 7. Circle of correlations between the molecular composition of the nests determined by pyrolysis and the land uses of the environments surrounding the nests. CHL=crops; CNF=conifers; EDF=buildings; FDC=deciduous; FDP=evergreen deciduous; MTR=kill; PRD=meadows; SDN=soil without vegetation; ZDM=scorched land.

In conclusion, our study shows an association between the presence of different types of guaiacols and pines (CNF). The same occurs between syringols and angiosperms (FDC and FDP), which is in agreement with current knowledge of the molecular composition of wood. Hence, the molecular composition of the nests is related to the surrounding vegetation, even though this association does not *control* the variation in lignin chemistry. In fact, the results indicate that *V. velutina* has a high flexibility in the use of the environment. It does not show a pattern of preference for a certain type of vegetation but adapts to the materials it has available in its environment. The most likely situation is the joint use of angiosperms and gymnosperms for the manufacturing of the nest, and the horizontal stripes patterns probably relate to short-term variations in material preference. The analyses presented here establish the consideration that the natural forests are used at least as part of the source of raw material by the pulp forage collectors. However, there are other sources of materials (wood in construction, stored firewood, etc.) that do not necessarily coincide with the local vegetation, and this may be a major cause of variation in nest composition.

4. Conclusions

The novelty of this study lies in the fact that, for the first time, information on the molecular composition of *V. velutina* nests was obtained using analytical pyrolysis techniques. Pyrolysis-GC-MS is a fast screening method for paper envelope nest composition of social wasps and hornets. This preliminary study shows that, with some minor adaptations to the Py-GC-MS method, and use of complementary THM-GC-MS, these techniques can generate a wealth of information in paper envelope construction processes.

The Asian hornet nest envelopes produced mainly carbohydrate products (mostly from holocellulose and hemicellulose polysaccharides) and lignin products upon pyrolysis, both of which originate from vegetal forage materials, although there is a high number of other compounds that appear in minority quantities. There is a high compositional variability in the nests studied. The sections of the nests (envelope, combs, pedicel meconium) differ widely in terms of molecular composition.

The analysis of the envelopes of the nests reveals a high compositional variability, where differences in the presence of lignin of the guaiacol and syringol types can be seen and that these differences are associated with different types of vegetation. The banding observed in the envelope in the nests has low S/G ratios in the dark/reddish areas while the ratios are high in the case of the light bands. This indicates that the light bands are made of predominantly angiosperm material while the dark bands are made of gymnosperm material (wood and/or bark) or angiosperm bark. The multivariate analysis of the compositional data in relation to the predominant vegetation types around the nests indicates an association between the presence of guaiacols and coniferous forests (gymnosperms) and between the presence of syringols and that of broadleaf trees (angiosperms). Also, it seems that higher concentrations of polysaccharides are associated with the presence of evergreen trees (eucalypt, among others).

The Asian hornet does not seem to show a clear pattern of preference for a certain type of vegetation. Instead, it adapts to the materials available in its environment and utilizes them according to its convenience in nest construction. This highlights the high flexibility of the Asian wasp in utilizing the resources of the environment it colonizes. Conducting such studies contributes to a better understanding of the specific behavior of *V. velutina*, which, in turn, helps define appropriate actions to limit its expansion.

Acknowledgments

We are grateful to the teams of the Fire Service of Santiago de Compostela and the Brión Supramunicipal Emergencies Group (GES) for their support in the collection of nests, for their willingness to help, their effort and involvement. The Diputación de A Coruña is thanked for financial resources (Project code 2017-CP006).

References

Challinor, J.M., 2001. Review: the development and applications of thermally assisted hydrolysis and methylation reactions. Journal of Analytical and Applied Pyrolysis 61, 3-34.

Espelie, K.E., Himmelsbach, D.S., 1990. Characterization of pedicel, paper, and larval silk from nest of *Polistes annularis* (L.). Journal of Chemical Ecology 16(12), 3467-77.

Feás Sánchez, X., Charles, R.J., 2019. Notes on the nest architecture and colony composition in winter of the yellow-legged Asian hornet, *Vespa velutina* Lepeletier 1836 (Hym.: Vespidae), in its introduced habitat in Galicia (NW Spain). Insects 10(8), 237; https://doi.org/10.3390/insects10080237.

Hedges, J.I., Mann, D.C., 1979. The characterization of plant tissues by their lignin oxidation products. Geochim. Cosmochim. Acta 43, 1803–1807.

Kaal, J. Martinez-Cortizas, A., Biester, H. 2017. Downstream changes in molecular composition of DOM along a headwater stream in the Harz mountains (Central Germany) as determined by FTIR, Pyrolysis-GC–MS and THM-GC–MS. Journal of Analytical and Applied Pyrolysis 126, 50-61.

Kaal, J., Plaza, C., Pérez-Rodríguez, M., Biester, H., 2020. Towards understanding ecological disaster in the Harz Mountains (Central Germany) by carbon tracing: pyrolysis-GC-MS of biological tissues and their water-extractable organic matter (WEOM). Analytical Pyrolysis Letters, APL008, 1-17.

Lourenço, A., Rencoret, J., Chemetova, C., Gominho, J.; Gutiérrez Suárez, A., Del Río Andrade, J.C., Pereira, H., 2016. Lignin composition and structure differs between xylem, phloem and phellem in *Quercus suber* L. Frontiers in Plant Science 7, 1212.

Neiva, D.M., Rencoret, J., Marques, G., Gutiérrez, A., Gominho, J., Pereira, H., del Río, J.C.,2020. Lignin from tree barks: Chemical structure and valorization. ChemSusChem 13, 4537– 4547. doi: 10.1002/cssc.202000431.

Pazos, T., Álvarez-Figueiró, P., Cortés-Vázquez, J.A., Jácome, M.A., Servia, M.J., 2022. Of fears and budgets: Strategies of control in *Vespa velutina* iInvasion and lessons for best management practices. Environmental Management 70, 605–617.

Rodríguez-Flores, M.S., Seijo-Rodríguez, A., Escuredo, O., Seijo-Coello, M.C., 2019. Spreading of *Vespa velutina* in northwestern Spain: influence of elevation and meteorological factors and effect of bait trapping on target and non-target living organisms. Journal of Pest Science 92, 557–565.

Rome, Q., Dambrine, L., Onate, C., Muller, F., Villemant, C., García-Pérez, A.L., Maia, M., Carvalho-Esteves, P., Bruneau, E., 2013. Spread of the invasive hornet *Vespa velutina* Lepeletier, 1836, in Europe in 2012 (Hym. Vespidae). Bulletin de la Société entomologique de France Année 2013 118, 21-22.

Santos, R.B., Capanema, E.A., Ballakshin, M.Y., Chang, H.-M., Jameel, H., 2012. Lignin structural variation in hardwood species. Journal of Agricultural and Food Chemistry 60, 4923–4930.

Schmolz, E., Brüders, N., Daum, R., Lamprecht, I., 2000. Thermoanalytical investigations on paper covers of social wasps. Thermochimica Acta 361, 121-129.

Traoré, M., Kaal, J., Martínez Cortizas, A., 2017. Potential of pyrolysis-GC-MS molecular fingerprint as a proxy of Modern Age Iberian shipwreck wood preservation. Journal of Analytical and Applied Pyrolysis 126, 1-13.

Wenzel, J.W, 2020. Nest Structure: Social Wasps. In: Encyclopedia of Social Insects, C. Starr (Ed). doi:10.1007/978-3-319-90306-4_146-1 .

Appendix 1. List of Py-GC-MS products used for the semi-quantitative assessment of paper envelope composition. RT=retention time, *m/z*=mass/charge ratio, group = macromolecular source allocation: CARB=carbohydrate products (polysaccharides), PHEN=phenols and catechols, LIG=lignin products (G=guaiacols, S=syringols), MCC=methylene chain compounds (fatty acids).

#	Pyrolysis product	*m/z*	group	RT (min)	% (average)	SD
1	acetic acid	60	CARB	1.441	16.15	7.04
2	3/2-furaldehyde	95+96	CARB	1.977	4.94	1.42
3	2,3-dihydro-5-methylfuran-2-one	98+55	CARB	2.389	4.76	2.46
4	phenol	94+66	PHEN	2.822	1.67	0.68
5	4-hydroxy-5,6-dihydro-(2*H*)-pyran-2-one	114+58	CARB	2.736	6.27	2.24
6	2-hydroxy--3-methyl-2-cyclopenten-1-one	55+112	CARB	2.946	1.68	0.77
7	4-methylphenol	107+108	PHEN	3.292	1.14	0.45
8	guaiacol	109+124	LIG G	3.337	3.26	1.66
9	4-methylguaiacol	123+138	LIG G	3.956	1.81	1.08
10	1,4:3,6-dianhydro-α-D-glucopyranose	69+57	CARB	4.220	1.99	0.66
11	catechol	110	PHEN	4.404	2.47	1.19
12	4-ethylguaiacol	137+152	LIG G	4.516	0.77	0.43
13	methoxycatechol	125+140	PHEN	4.603	1.30	0.56
14	4-vinylguaiacol	150+135	LIG G	4.764	3.81	1.94
15	unidentified compound	57+73	OTHER	4.916	1.51	0.44
16	syringol	154+139	LIG S	5.011	2.46	1.33
17	4-(prop-1-enyl)guaiacol	164+149	LIG G	5.032	0.37	0.14
18	4-(prop-2-enyl)guaiacol (*trans*)	164+149	LIG G	5.633	1.92	0.81
19	homovanillin	137+166	LIG G	5.018	0.20	0.11
20	vanillin	151+152	LIG G	5.472	1.11	0.45
21	4-methylsyringol	168+153	LIG S	5.617	1.71	0.86
22	4-acetylguaiacol	151+166	LIG G	5.971	1.11	0.42
23	4-ethylsyringol	167+182	LIG S	6.091	0.56	0.27
24	4-(propan-2-one)guaiacol	137+180	LIG G	6.210	0.67	0.35
25	4-vinylsyringol	180+165	LIG S	6.338	3.27	1.86
26	4-propylsyringol	167+196	LIG S	6.598	0.24	0.13
27	homosyringaldehyde	167+196	LIG S	7.076	0.12	0.07
28	4-(prop-1-enyl)syringol	194+179	LIG S	6.540	0.38	0.18
29	4-(prop-2-enyl)syringol (*cis*)	194+179	LIG S	6.808	0.24	0.13
30	4-(prop-2-enyl)syringol (*trans*)	194+179	LIG S	7.055	2.38	1.50
31	levogalactosan	60+73	CARB	5.803	2.77	1.29

32	levomannosan	60+73	CARB	6.198	2.61	1.26
33	levoglucosan	60+73	CARB	6.773	19.94	8.12
34	syringaldehyde	181+182	LIG S	6.977	0.56	0.29
35	4-acetylsyringol	181+196	LIG S	7.282	0.82	0.49
36	4-(propan-2-one)syringol	167+210	LIG S	7.410	1.05	0.61
37	4-(propan-3-one)syringol	181+210	LIG S	7.604	0.44	0.25
38	dihydrosinapyl alcohol	168+212	LIG S	7.880	0.18	0.13
39	sinapyl aldehyde (*trans*)	137+208	LIG S	8.185	0.38	0.29
40	C_{16}-fatty acid	60+73	MCC	7.936	0.68	0.43
41	C_{18}-fatty acid	60+73	MCC	8.457	0.13	0.11
42	unidentified compound	83+280	OTROS	8.840	0.15	0.11